Diagn Interv Radiol 2023; DOI: 10.5152/dir.2022.21562

BREAST IMAGING

ORIGINAL ARTICLE

Contrast-enhanced spectral mammography: are kinetic patterns useful for differential diagnoses of enhanced lesions?

Xiaocui Rong
Yihe Kang
Jing Xue
Pengyin Han
Guang Yang
Zhigang Li

PURPOSE

To investigate the diagnostic efficiency of the kinetic curves of enhanced lesions on contrast-enhanced spectral mammography (CESM) and whether they were similar to those of magnetic resonance imaging (MRI).

METHODS

Two hundred and twelve patients with 222 enhanced lesions were included in this prospective study. Single-view craniocaudal of an affected breast was acquired at 3, 5, and 7 min after contrast media injection. The kinetic patterns of each lesion were evaluated and classified as elevated (type I), steady (type II), and depressed (type III). Statistical comparison used the chi-squared test, the receiver operating characteristic (ROC) curve, and Cohen's kappa.

RESULTS

Of 222 enhanced lesions, 140 were breast cancers, and 82 were benign lesions. The distribution of the kinetic curves for breast cancer was type I, 3.57%, type II, 35.71%, and type III, 60.72%. As for benign lesions, the distribution was type I, 43.90%, type II, 45.12%, and type III, 10.98%. The difference in the enhancement patterns between benign lesions and breast cancers was significant ($P < 0.001$). The likelihood of breast cancer related to a type I, II, and III curve was 12.20%, 57.47%, and 90.43%, respectively. For the enhancement intensity, the area under curve (AUC) of the ROC curves was 0.702 ± 0.036; for enhancement patterns, the AUC increased to 0.819 ± 0.030. Cohen's kappa coefficient was 0.752 ($P < 0.001$) regarding the kinetic curves for CESM and MRI.

CONCLUSION

The kinetic patterns on CESM show promise in differentiating between benign lesions and breast cancers, with good agreement, when compared with MRI.

KEYWORDS

Breast cancer, contrast-enhanced spectral mammography, contrast agents

Breast cancer is now the most common cancer and the main cause of cancer-related death in women. About 2.3 million new breast cancer cases are diagnosed worldwide, accounting for nearly 25% of all cancer cases among females.[1] Full-field digital mammography (FFDM) and digital breast tomosynthesis are widely used in the screening and diagnosis of breast cancer, but some tumors, surrounded mostly by glandular tissue, might be missed with both techniques.[2] Ultrasound is a commonly used imaging examination for dense breasts, but its diagnostic efficacy is operator-dependent.[3]

Traditionally, dynamic contrast-enhanced magnetic resonance imaging (DCE-MRI) has been considered a sensitive imaging examination for breast cancer detection, and the types of the time-intensity curve (TIC) can be used as differential diagnostic criteria for breast-enhancing lesions.[4,5] However, DCE-MRI has a lengthy examination time and a relatively large number of false positive results, leading to additional examinations and biopsies. It is also

From the Department of Radiology (X.R., Y.K., J.X., P.H., G.Y., Z.L. ✉ zhigangli050011@163.com), Hebei Medical University Fourth Affiliated Hospital, Shijiazhuang, China.

Received 15 June 2021; revision requested 14 July 2021; last revision received 21 December 2021; accepted 27 December 2021.

Epub: 27.02.2023

Publication date:

DOI: 10.5152/dir.2022.21562

You may cite this article as: Rong X, Kang Y, Xue J, Han P, Yang G, Li Z. Contrast-enhanced spectral mammography: are kinetic patterns useful for differential diagnoses of enhanced lesions? Diagn Interv Radiol. 27 February 2023 DOI: 10.5152/dir.2022.21562 [Epub Ahead of Print].

expensive and not available for all patients.[6] Contrast-enhanced spectral mammography (CESM) is a promising new technology. Similar to MRI, CESM reflects the angiogenesis associated with breast cancer. Fallenberg et al.[7] and Kim et al.[8] showed that CESM and MRI had comparable accuracy for breast cancer detection. Clauser et al.[9] also demonstrated that CESM had a higher specificity than MRI. However, some benign enhanced lesions such as fibroadenomas, papillomas, hamartomas, intra-mammary nodes, and fat necrosis were misdiagnosed as breast cancer on CESM.[10,11] CESM is a suitable alternative to MRI if it can provide morphological and kinetic information equivalent to DCE-MRI.

This pilot study aims to evaluate the diagnostic efficacy of kinetic curves of enhanced lesions on CESM and whether they are similar to those on MRI.

Methods

Patients

This prospective study was approved by the Fourth Hospital of Hebei Medical University ethics committee (no: 2020KY182). Written informed consent was obtained from all patients. The inclusion criteria were: (1) suspected lesions determined by breast sonography, mammography, or both; (2) all breast lesions confirmed by pathology via either percutaneous breast core needle biopsy or excision surgery; (3) cases where CESM were conducted according to our standardized protocol: conducting craniocaudal (CC) views of the normal breast first and CC views of the affected breast later acquired at 3, 5, and 7 min after a contrast agent injection. Patients who did not meet the inclusion criteria and those who met the following exclusion criteria were not accepted to this study: contraindications to iodinated contrast media and poor image quality. As the study flow chart (Figure 1) shows, a total of 212 patients (mean age, 48.09 ± 10.17 years; range, 21–74 years) with 222 lesions were included in this study from April 2019 to June 2020.

Main points

- The kinetics of the contrast agent can be evaluated using contrast-enhanced spectral mammography (CESM).
- Contrast agent kinetic patterns on CESM show good performance in differentiating between benign and malignant breast-enhanced lesions.
- The kinetic patterns on CESM are similar to those on magnetic resonance imaging.

Image acquisition and assessment

CESM

CESM was conducted using the Senographe Essential (GE Healthcare), which is equipped with an amorphous silicon flat panel detector. All patients received an intravenous injection of iodine contrast media (370 mg iodine/mL, 1.22 mL/kg body weight, flow rate 3 mL/s) through the antecubital vein. Two min after the injection, bilateral breast images were obtained by the sequence of contralateral CC projection, and ipsilateral CC projection acquired at 3 (a relatively early phase), 5, and 7 min (a relatively late phase) with the breast compressed after a contrast agent injection. For each exposure, both the low-energy and high-energy images were obtained. The recombined images were acquired by automated post-processing. In the recombined CESM images, a region of interest (ROI) was manually delineated by two radiologists (readers A and B), and the signal values of enhanced lesions and the percentage signal difference between the enhanced lesion and the background (%RS), according to the enhancement formula (S'c – S'b) / S'b × 100%,[12] were measured to evaluate enhancement intensity, where S'c and S'b were signal values in the ROI of the breast lesion and the background, respectively. The enhancement formula (%RS1 – %RS2) / %RS2 × 100% was applied to calculate the value of the pattern of kinetics curves, where %RS1 and %RS2 were %RS values measured in the CC projection at 3 and 7 min after the injection, respectively. An ROI was selectively placed in the areas of the breast lesion with the fastest and strongest enhancement, and its size varied with the size of the enhanced lesion ranging from 5 to 216 mm^2. Attention was given to keeping the ROI in the same location of the lesion and at the exact sizes at each time point to ensure the accuracy of the curve measurement. The ROI of the background was placed in an area of the most homogeneous fatty tissue, far away from the enhanced focus or breast parenchyma. The enhancement intensity was measured at the first postcontrast image (3 min). The patterns of the kinetic curve were classified into three categories: (1) type I, elevated pattern (the enhancement increased more than 10%), (2) type II, steady pattern (the enhancement changed within 10%), and (3) type III, depressed pattern (the enhancement decreased more than 10%) (Figure 2).

MRI

All breast MRI examinations were conducted on a 1.5T MR scanner (Signa HDe, GE Healthcare) with dedicated phased-array breast-surface coils. Patients were in a prone position, with naturally sagging breasts. The DCE-MRI was performed using volume imaging for the breast assessment (VIBRANTI) and fat-suppressed technology with the following scanning parameters: repetition time 5.6 ms, echo time 1.0 ms, the field of view 320 mm, flip angle 15°, matrix 320 × 288, slice

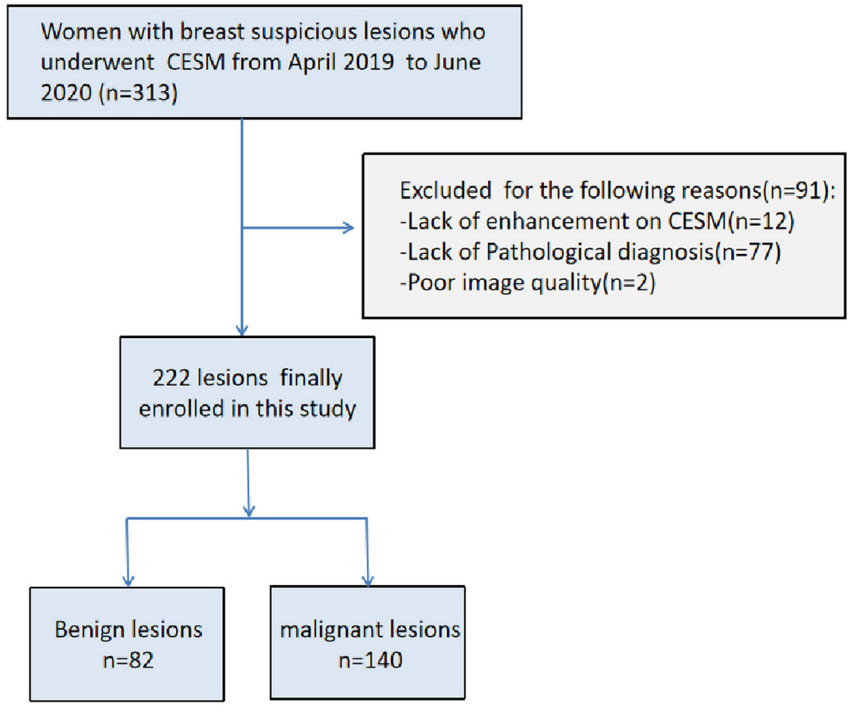

Figure 1. The flow of the study. CESM, contrast-enhanced spectral mammography.

thickness 1.2 mm without an intersection gap, and an imaging time of 62 s per dynamic image. The dynamic series included eight dynamic images: one was acquired before and seven following a 30 s delay after the intravenous injection of Gadoterate meglumine (0.1 mmoL/kg body weight) at a flow rate of 3 mL/s. The MRI-enhanced images were acquired between 1 min and 7 min 12 s.

Statistical analysis

Data analysis and graphical work were performed using SPSS Statistics (version 21.0, IBM, Armonk, NY) and GraphPad Prism 8.0. The Kolmogorov–Smirnov test was used to assess the normality of the data. Descriptive data statistics were presented with n (%), and normal distributions were shown as mean ± standard deviation. The independent samples t-test and the One-Way analysis of variance were used to compare the difference in enhancement degree (%RS) in different lesion types, followed by multiple comparisons using the least significant difference test. A chi-squared test was used to test the significance of the curve-type distribution in benign and malignant breast lesions. The receiver operating characteristic (ROC) analysis was performed to evaluate the diagnostic performance of enhancement intensity and patterns on the CESM, and the areas under the curve (AUCs) were calculated and shown as AUC ± standard error. The best cut-off value was determined using the Youden index. Qualitative agreement between CESM and MRI and the inter-reader agreement in contrast agent kinetics were analyzed using Cohen's kappa. A kappa coefficient of ≤0.20 indicated poor agreement; 0.21–0.40, fair agreement; 0.41–0.60, moderate agreement; 0.61–0.80, good agreement; and >0.80, excellent agreement.[13] For all tests, a two-sided *P* value of <0.050 was considered statistically significant.

Results

Diagnosis of lesions

Of the 222 enhanced lesions, 140 (63.06%) were breast cancers, consisting of 116 (52.25%) infiltrating cancers and 24 (10.81%) non-infiltrating cancers (ductal carcinoma *in situ*). The infiltrating cancers included 104 invasive ductal cancers not otherwise specified, 8 papillary carcinomas, 1 metaplastic carcinoma, 1 apocrine carcinoma, 1 mucinous cancer, and 1 invasive lobular cancer. Of the 82 (36.94%) benign lesions, 24 were adenosis, 23 fibroadenomas, 19 intraductal papillomas, 11 inflammatory lesions, 3 cysts with infection, 1 phyllodes tumor, and 1 myofibroblastic neoplasia. All the diagnoses were confirmed by core needle biopsy or excisional biopsy.

Enhancement intensity on CESM

The comparison of %RS by lesion type is presented in Figure 3. In the malignant lesion group, the mean %RS was 4.50 ± 2.20 (4.77 ± 2.18 for infiltrating cancers, 3.58 ± 2.02 for non-infiltrating cancers), while in the benign lesion group, the mean %RS was 3.19 ± 1.81. The comparison between %RS for the benign and malignant groups was statistically significant ($P < 0.001$). There was a significant statistical difference in %RS among the benign lesions, non-infiltrating cancers, and infiltrating cancers groups ($P < 0.001$, Table 1). The %RS of infiltrating cancers was higher than non-infiltrating and benign lesions ($P = 0.004$, $P < 0.001$). There was no significant difference between %RS for the non-infiltrating cancers and benign lesions ($P = 0.337$).

Enhancement patterns of CESM

Among breast cancers, a type III curve accounted for 60.72% (85 of 140), a type II curve for 35.71% (50 of 140), and a type I curve for 3.57% (5 of 140). As for benign lesions, a type I curve occurred in 43.90% (36 of 82), a type II curve was seen in 45.12% (37 of 82), and a type III curve presented in 10.98% (9 of 82). The difference in enhancement patterns between malignant and benign lesions was significant ($P < 0.001$, Table 2). Table 3 provides the enhancement patterns of CESM in differ-

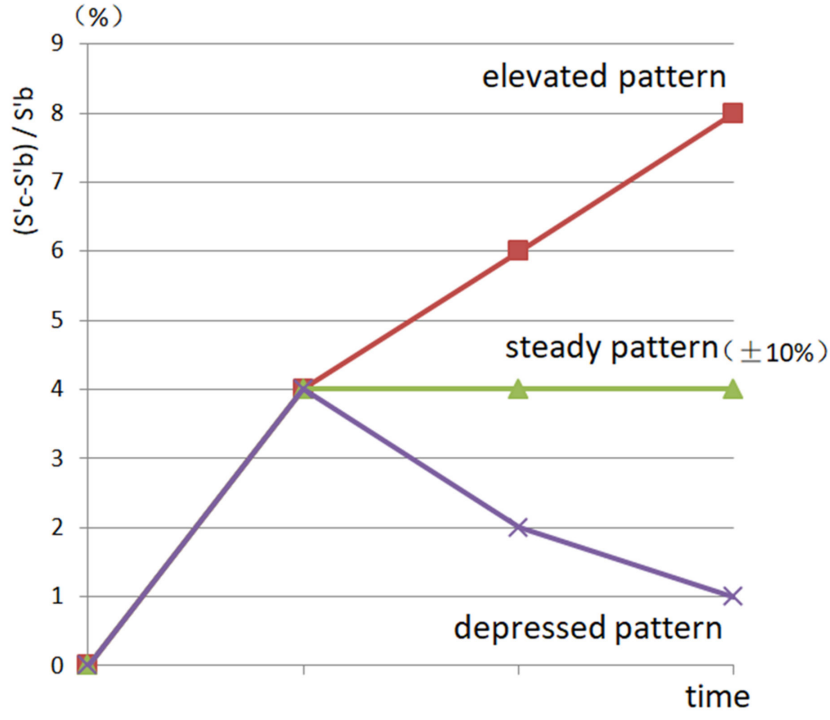

Figure 2 The patterns of the kinetic curve. Any change from −10% to 10% was considered a steady pattern, more than 10% was considered an elevated pattern, and less than −10% was considered a decreased pattern.

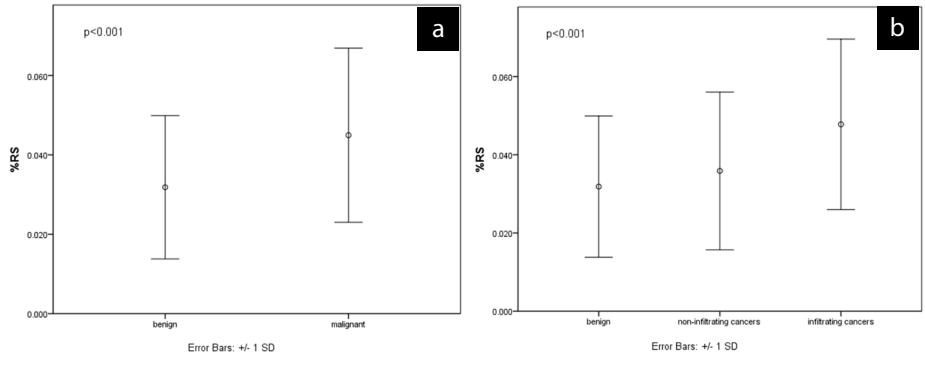

Figure 3. (a, b) Comparison of %RS with lesion type. SD, standard deviation.

Table 1. Descriptive and multiple comparison statistics

	Type of lesion			*P* (ANOVA)	*P* (LSD)		
	Benign (A)	Non-infiltrating cancers (B)	Infiltrating cancers (C)		A vs. B	A vs. C	B vs. C
%RS (mean ± SD)	3.19 ± 1.81	3.58 ± 2.02	4.77 ± 2.18	<0.001	0.337	<0.001	0.004

A, benign; ANOVA, One-Way analysis of variance; B, non-infiltrating cancers; C, infiltrating cancers; LSD, least significant difference; SD, standard deviation.

Table 2. Kinetic patterns on CESM between benign and malignant breast lesions

Kinetic pattern	Benign lesions n (%)	Malignant lesions n (%)	*P* value
Type I	36 (43.90)	5 (3.57)	
Type II	37 (45.12)	50 (35.71)	<0.001
Type III	9 (10.98)	85 (60.72)	

CESM, contrast-enhanced spectral mammography.

Table 3. Enhancement patterns on CESM in different histopathological results

Type of lesion		Type of curve			
		Type I n (%)	Type II n (%)	Type III n (%)	Total n (%)
Benign	Adenosis	8 (22.22)	15 (40.54)	1 (11.11)	24 (29.27)
	Fibroadenoma	16 (44.44)	4 (10.81)	3 (33.33)	23 (28.05)
	Intraductal papilloma	4 (11.11)	11 (29.73)	4 (44.45)	19 (23.17)
	Inflammatory lesion	4 (11.11)	6 (16.22)	1 (11.11)	11 (13.41)
	Cysts with infection	3 (8.34)	0 (0.00)	0 (0.00)	3 (3.66)
	Phyllodes tumor	0 (0.00)	1 (2.70)	0 (0.00)	1 (1.22)
	Myofibroblastic neoplasia	1 (2.78)	0 (0.00)	0 (0.00)	1 (1.22)
Total		36	37	9	82
Malignant	Invasive ductal cancer	2 (40.00)	30 (60.00)	72 (84.70)	104 (74.29)
	Ductal carcinoma in situ	3 (60.00)	15 (30.00)	6 (7.06)	24 (17.15)
	Papillary carcinoma	0 (0.00)	3 (6.00)	5 (5.88)	8 (5.72)
	Metaplastic carcinoma	0 (0.00)	0 (0.00)	1 (1.18)	1 (0.71)
	Apocrine carcinoma	0 (0.00)	0 (0.00)	1 (1.18)	1 (0.71)
	Mucinous cancer	0 (0.00)	1 (2.00)	0 (0.00)	1 (0.71)
	Invasive lobular cancer	0 (0.00)	1 (2.00)	0 (0.00)	1 (0.71)
Total		5	50	85	140

CESM, contrast-enhanced spectral mammography.

ent histopathological results. The likelihood of breast cancer related to a type I, II, and III curve was 12.20% (5 of 41), 57.47% (50 of 87), and 90.43% (85 of 94), respectively.

The ROC analysis results

For the enhancement intensity, the AUC was 0.702 ± 0.036 [95% confidence interval (CI) from 0.631 to 0.773, $P < 0.001$]. According to the Youden index, the optimal cut-off value of %RS for the differentiation between benign and malignant lesions was 3.60, sensitivity was 64.00%, specificity was 72.00%, accuracy was 66.20%, positive likelihood ratio was 2.14, and negative likelihood ratio was 0.50. For enhancement patterns, the AUC increased to 0.819 ± 0.030 (95% CI from 0.761 to 0.877, $P < 0.001$). Figure 4 shows the ROC curves. The difference between the two AUC values was statistically significant ($P < 0.001$).

Inter-reader variability of enhancement pattern classification

In 91.89% (204 of 222) of cases, the two readers had consistent results in enhancement patterns. In the 18 (8.11%) cases with inconsistent classification, there were differences between type I and type II or type II and type III. There was no difference in classification between type I and type III (Table 4). The kappa coefficient was 0.873 ($P < 0.001$), indicating excellent inter-reader agreement.

Comparison of enhancement patterns in CESM and MRI

One hundred twenty patients with 120 lesions underwent CESM and MRI examination. Comparing the types of kinetic curves on CESM and MRI, the results showed that the accordance rate between the two examination methods was 85.00%, of which 10.00% (12 of 120) were type I curve, 35.83% (43 of 120) were type II, 39.17% (47 of 120) were type III (Figure 5), and the other 15.00% (18 of 120) had inconsistent kinetic curves (Table 5). Cohen's kappa coefficient for CESM and MRI was 0.752 ($P < 0.001$), indicating good agreement (0.6–0.8).

Discussion

The CESM technique is an emerging modality that combines traditional mammography with administering an intravenous contrast agent and is increasingly being used in diagnostics to differentiate benign lesions from breast cancers. Most malignant lesions are hypervascular, with immature tumor blood vessels. Hence, malignant lesions usually exhibit earlier and stronger enhancement than benign lesions.[4,14] This study showed a significant correlation between a lesion's enhancement intensity (%RS) on CESM and malignancy. The enhancement intensity of benign lesions was lower than that of malignant tumors, and the degree of enhancement of benign lesions and non-invasive cancers was lower than invasive cancers, consistent with the results of Rudnicki et al.[12,15] Nonetheless, the diagnostic efficiency is low (accuracy was 66.20%, AUC was 0.702 ± 0.036) if the differentiation between benign and malignant lesions depends on the enhancement intensity. To further improve the diagnostic efficiency of CESM, this study investigated enhancement patterns on CESM between benign lesions and breast cancers. The preliminary research indicated that the difference in enhancement patterns on CESM between malignant and benign lesions was significant, and the AUC was 0.819 ± 0.030. In breast cancers, the steady or depressed patterns (type II or III) were dominant. On the contrary, benign lesions mainly showed an elevated and steady pattern (type I or II). According to the results of this study, the likelihood of breast cancer related to a type III curve was 90.43%, whereas the likelihood of breast cancer related to a type I curve was only 12.20%.

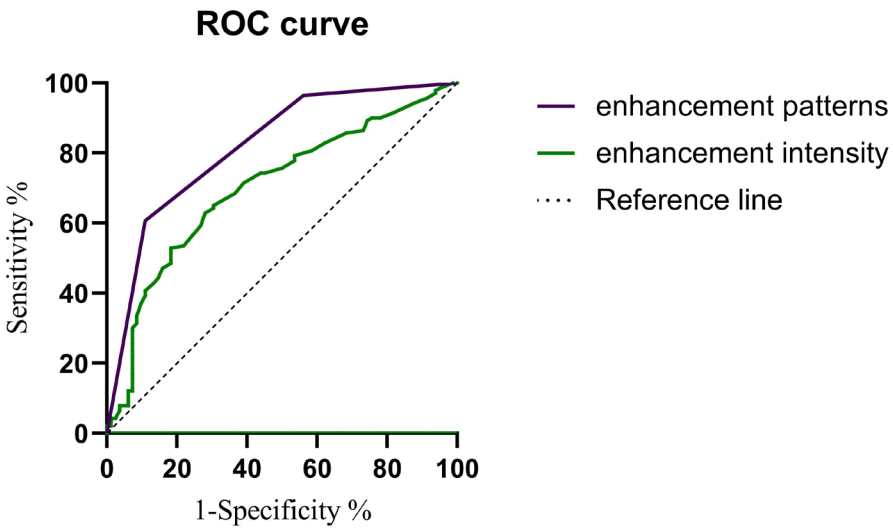

Figure 4. Receiver operating characteristic curves for enhancement intensity and enhancement patterns. ROC, receiver operating characteristic.

Table 4. Comparison of enhancement patterns between reader 1 and reader 2

Reader 1	Reader 2			Total
	Type I	Type II	Type III	
Type I	41	1	0	42
Type II	2	78	9	89
Type III	0	6	85	91
Total	43	85	94	222

Until now, there have been only a few studies about the kinetic investigation of CESM. Jong et al.[16] and Dromain et al.[17] conducted a small sample study using a temporal subtraction method instead of a dual-energy approach to CESM. In their studies, a mask image and a post-contrast image were obtained before and after the injection of a contrast agent, and a subtraction image was derived from imaging post-processing. Their technique was more susceptible to motion. Jong et al.[16] showed that 4 of 10 (40%) breast cancer lesions had a plateau curve, 3 of 10 (30%) presented with a washout curve, 1 of 10 (10%) had increasing enhancement, and 2 of 10 (20%) had no enhancement. Due to a limited number of patients, statistical significance was not measured in that study. In the study by Dromain et al.[17], they acquired the images from 30 s to 7 min and considered early if the enhancement peak was before 1 min 30 s. In their few cases, gradually increasing enhancement (35%, 7/20) was the most common kinetic curve observed in breast cancers, and a washout curve was only found in 20% of cases. They considered that the discrepancy between kinetic curves observed using CESM and MRI might be due to the compression of the breast, which may alter blood flow. In addition, the different kinetic patterns may be caused by the difference in acquisition times. Recent studies[18-20] showed that the comparison of enhancement patterns on CESM between malignant and benign lesions was significant. Deng et al.[18] used the time interval between the CC projection and mediolateral (MLO) projection to assess relative enhancement patterns. Among the relative enhancement patterns, the incidence of malignant and benign lesions was 73.08% (19/26) and 26.92% (7/26) in the elevated pattern, 92.86% (13/14) and 7.14% (1/14) in the steady pattern, 94.29% (66/70) and 5.71% (4/70) in the depressed pattern, and 20.0% (32/40) and 80.00% (8/40) in non-enhancement lesions, respectively. Liu et al.[19] also evaluated the enhancement patterns based on two different views of CC and MLO. This may affect the results since the tissues superimposed and adjacent to the lesions will be different in different positions. Reported in their study was an accordance rate of 64.2% for enhancement patterns on CESM and MRI. The study by Huang et al.[20] demonstrated that the washout pattern was significantly associated with malignant lesions at 2–4 and 2–10 min frames based on two readers' interpretations. However, they did not evaluate the diagnostic efficacy of enhancement patterns on CESM in detail, nor did they compare it with TIC on MRI. All images in that study were obtained on MLO view without releasing the paddle. The enhancement of suspicious lesions was semi-quantitatively analyzed using a 10-point grayscale reference bar.

In the present study, the CC view was used because it was easier for the patients to remain motionless in this projection.[16,17] The patients' motion can cause faulty kinetic curves. Thus, care was taken to keep the ROI at the same position of the lesion at each imaging time point.[21] Only three CC views were performed on the affected breast to reduce the patients' radiation dose. Because the signal value differences of the lesions at different time points after enhancement were small in absolute values, and the pre-contrast signal values on the recombined images of breast lesions were roughly equal to the post-contrast signal values of background, the %RS on CESM was used to make it comparable to DCE-MRI.[12]

Some studies have shown a significant correlation between enhancement patterns and a moderate agreement (Cohen's kappa coefficient was 0.438 and 0.515) between contrast-enhanced digital breast tomosynthesis or CESM and MRI.[19,22] By comparing the enhancement patterns of CESM and MRI, we found that the accordance rate of the two examination methods was 85.0%, and the agreement was good (Kappa coefficient: 0.752).

The present study had some limitations. Firstly, this study had a limited number of patients from a single institution. Nonetheless, the sample size in this study was the largest for kinetic curves on CESM. Secondly, the radiation dose of CESM was not considered. Previous studies have shown that the combined radiation dose estimated from low- and high-energy views is about 1.2 times that of conventional FFDM.[11,23] The dose values of CESM meet the recommendations for the maximum dose in mammography.[24] Although the radiation dose is increased, CESM provides radiologists with a standard low-energy image (similar to FFDM) and a recombined image highlighting angiogenesis areas. In the future, when a CESM examination is planned, additional FFDM can be avoided, with the possibility of saving up to 48.5% of the radiation dose (depending on the system used).[25] This study's authors plan to explore ways to reduce radiation doses in further studies. Thirdly, CESM was not arranged according to the patients' menstrual cycles. The background parenchymal enhancement may be more obvious in patients with CESM before menstruation, which will

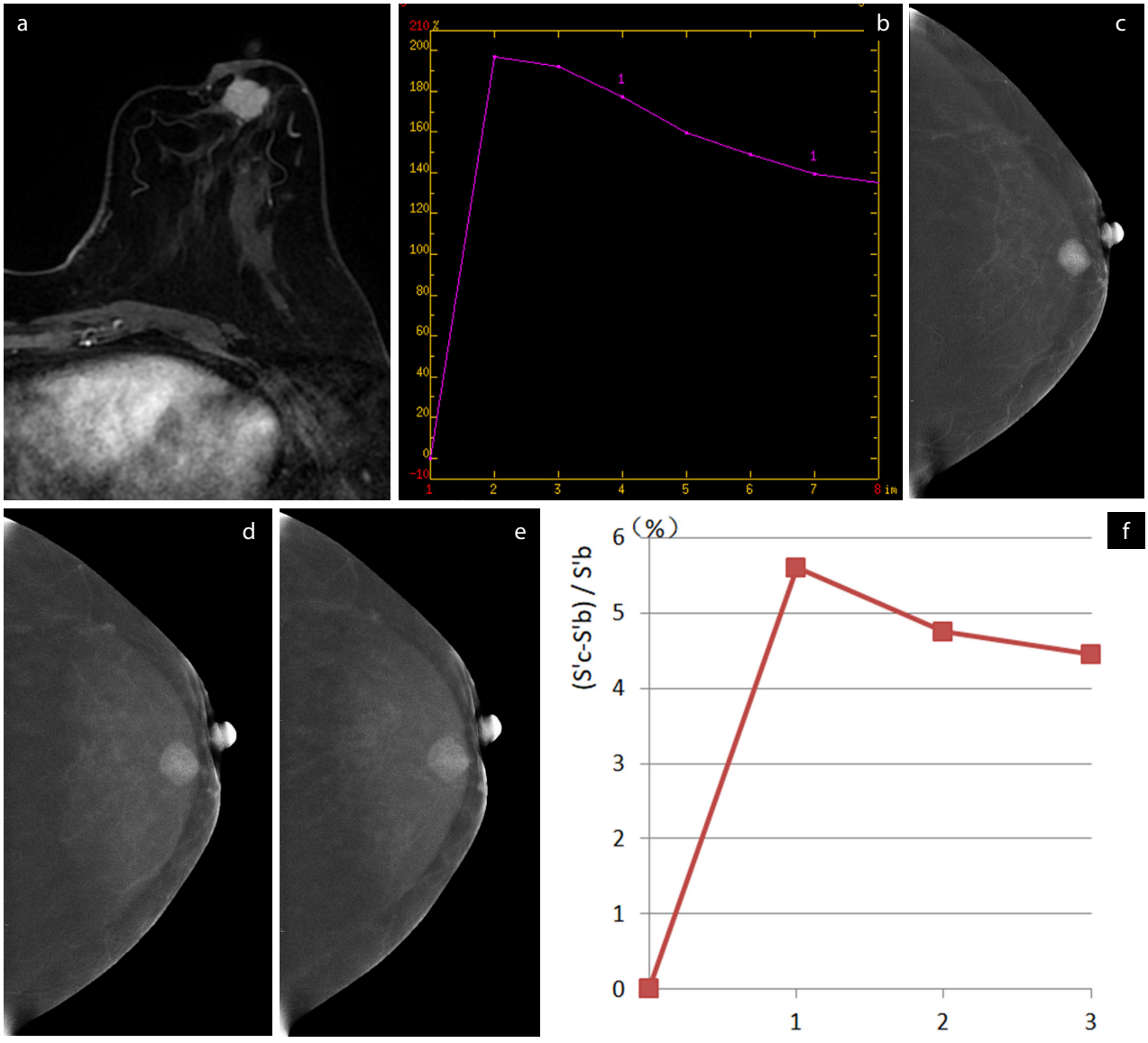

Figure 5. An invasive ductal carcinoma in the left breast of a 45-year-old woman. An early post-contrast magnetic resonance image depicts a strongly enhancing lesion (a). The time-signal intensity curve of the mass on magnetic resonance imaging shows a washout time course (b). The subtraction images of contrast-enhanced spectral mammography (CESM) obtained 3, 5, and 7 min after the contrast agent injection show a round circumscribed mass, and the enhancement intensity decreases with time **(c-e)**. The kinetic curve of contrast enhancement derived from the receiver operating characteristics drawn in this lesion on CESM shows a depressed pattern **(f)**.

Table 5. Comparison of enhancement patterns between CESM and MRI

CESM	MRI			Total
	Type I	Type II	Type III	
Type I	12	3	0	15
Type II	4	43	4	51
Type III	0	7	47	54
Total	16	53	51	120

CESM, contrast-enhanced spectral mammography; MRI, magnetic resonance imaging.

affect the accuracy of the measurement results. In addition, the enhancement patterns in breast cancers with different histopathology were not discussed because of the small number of patients in each subtype. Finally, there is no commercial tool for the quantitative analysis of the kinetic curve on CESM. The ROI was drawn manually, which was subjective and time-consuming. The inter- and intra-observer reproducibility may be poor. Nevertheless, this study demonstrated that the agreement was excellent (Kappa coefficient: 0.873) for the curve types between the two readers.

In conclusion, our results showed that the kinetic pattern of enhanced lesions on CESM effectively differentiates benign from malignant breast lesions, with good agreement, when compared with MRI.

Acknowledgments

The authors would like to thank Junjing Zhao and Xiujian Liu for their help in creating this article.

Conflict of interest disclosure

The authors declared no conflicts of interest.

References

1. Sung H, Ferlay J, Siegel RL, et al. Global Cancer Statistics 2020: GLOBOCAN estimates of incidence and mortality worldwide for 36 cancers in 185 countries. *CA Cancer J Clin.* 2021;71(3):209-249. [CrossRef]
2. Lee SH, Jang MJ, Kim SM, et al. Factors affecting breast cancer detectability on digital breast tomosynthesis and two-dimensional digital mammography in patients with dense breasts. *Korean J Radiol.* 2019;20(1):58-68. [CrossRef]
3. Abdullah N, Mesurolle B, El-Khoury M, Kao E. Breast imaging reporting and data system lexicon for US: interobserver agreement for assessment of breast masses. *Radiology.* 2009;252(3):665-672. [CrossRef]
4. Kuhl CK, Mielcareck P, Klaschik S, et al. Dynamic breast MR imaging: are signal intensity time course data useful for differential diagnosis of enhancing lesions? *Radiology.* 1999;211(1):101-110. [CrossRef]
5. Mann RM, Kuhl CK, Kinkel K, Boetes C. Breast MRI: guidelines from the European Society of Breast Imaging. *Eur Radiol.* 2008;18(7):1307-1318. [CrossRef]
6. Ghaderi KF, Phillips J, Perry H, Lotfi P, Mehta TS. Contrast-enhanced mammography: current applications and future directions. *Radiographics.* 2019;39(7):1907-1920. [CrossRef]
7. Fallenberg EM, Schmitzberger FF, Amer H, et al. Contrast-enhanced spectral mammography vs. mammography and MRI - clinical performance in a multi-reader evaluation. *Eur Radiol.* 2017;27(7):2752-2764. [CrossRef]
8. Kim EY, Youn I, Lee KH, et al. Diagnostic value of contrast-enhanced digital mammography versus contrast-enhanced magnetic resonance imaging for the preoperative evaluation of breast cancer. *J Breast Cancer.* 2018;21(4):453-462. [CrossRef]
9. Clauser P, Baltzer PAT, Kapetas P, et al. Low-dose, contrast-enhanced mammography compared to contrast-enhanced breast MRI: a feasibility study. *J Magn Reson Imaging.* 2020;52(2):589-595. [CrossRef]
10. James JJ, Tennant SL. Contrast-enhanced spectral mammography (CESM). *Clin Radiol.* 2018;73(8):715-723. [CrossRef]
11. Dromain C, Thibault F, Diekmann F, et al. Dual-energy contrast-enhanced digital mammography: initial clinical results of a multireader, multicase study. *Breast Cancer Res.* 2012;14(3):R94. [CrossRef]
12. Rudnicki W, Heinze S, Niemiec J, et al. Correlation between quantitative assessment of contrast enhancement in contrast-enhanced spectral mammography (CESM) and histopathology-preliminary results. *Eur Radiol.* 2019;29(11):6220-6226. [CrossRef]
13. Landis JR, Koch GG. The measurement of observer agreement for categorical data. *Biometrics.* 1977;33(1):159-174. [CrossRef]
14. Watt AC, Ackerman LV, Windham JP, et al. Breast lesions: differential diagnosis using digital subtraction angiography. *Radiology.* 1986;159(1):39-42. [CrossRef]
15. Rudnicki W, Heinze S, Popiela T, Kojs Z, Luczynska E. Quantitative assessment of contrast enhancement on contrast enhancement spectral mammography (CESM) and comparison with qualitative assessment. *Anticancer Res.* 2020;40(5):2925-2932. [CrossRef]
16. Jong RA, Yaffe MJ, Skarpathiotakis M, et al. Contrast-enhanced digital mammography: initial clinical experience. *Radiology.* 2003;228(3):842-850. [CrossRef]
17. Dromain C, Balleyguier C, Muller S, et al. Evaluation of tumor angiogenesis of breast carcinoma using contrast-enhanced digital mammography. *AJR Am J Roentgenol.* 2006;187(5):W528-W537. [CrossRef]
18. Deng CY, Juan YH, Cheung YC, et al. Quantitative analysis of enhanced malignant and benign lesions on contrast-enhanced spectral mammography. *Br J Radiol.* 2018;91(1086):20170605. [CrossRef]
19. Liu Y, Zhao S, Huang J, et al. Quantitative analysis of enhancement intensity and patterns on contrast-enhanced spectral mammography. *Sci Rep.* 2020;10(1):9807. [CrossRef]
20. Huang JS, Pan HB, Yang TL, et al. Kinetic patterns of benign and malignant breast lesions on contrast enhanced digital mammogram. *PLoS One.* 2020;15(9):e0239271. [CrossRef]
21. Kuhl CK, Jost P, Morakkabati N, Zivanovic O, Schild HH, Gieseke J. Contrast-enhanced MR imaging of the breast at 3.0 and 1.5 T in the same patients: initial experience. *Radiology.* 2006;239(3):666-676. [CrossRef]
22. Froeling V, Diekmann F, Renz DM, et al. Correlation of contrast agent kinetics between iodinated contrast-enhanced spectral tomosynthesis and gadolinium-enhanced MRI of breast lesions. *Eur Radiol.* 2013;23(6):1528-1536. [CrossRef]
23. Lobbes MB, Smidt ML, Houwers J, Tjan-Heijnen VC, Wildberger JE. Contrast enhanced mammography: techniques, current results, and potential indications. *Clin Radiol.* 2013;68(9):935-944. [CrossRef]
24. Jeukens CR, Lalji UC, Meijer E, et al. Radiation exposure of contrast-enhanced spectral mammography compared with full-field digital mammography. *Invest Radiol.* 2014;49(10):659-665. [CrossRef]
25. Fallenberg EM, Dromain C, Diekmann F, et al. Contrast-enhanced spectral mammography: does mammography provide additional clinical benefits or can some radiation exposure be avoided? *Breast Cancer Res Treat.* 2014;146(2):371-381. [CrossRef]